Chinese Chemical Letters 31 (2020) 1193–1196

Contents lists available at ScienceDirect

Chinese Chemical Letters

journal homepage: www.elsevier.com/locate/cclet

Communication

# B←N-containing azaacenes with propynyl groups on boron atoms

Linan Li[a], Ying Gao[a,*], Chuandong Dou[b,*], Jun Liu[b,*]

[a] School of Chemistry and Environmental Engineering, Changchun University of Science and Technology, Changchun 130022, China
[b] State Key Laboratory of Polymer Physics and Chemistry, Changchun Institute of Applied Chemistry, Chinese Academy of Sciences, Changchun 130022, China

ARTICLE INFO

*Article history:*
Received 26 September 2019
Received in revised form 2 November 2019
Accepted 11 November 2019
Available online 12 November 2019

*Keywords:*
Polyarene
Azaacene
B-N coordination bond
NIR absorption
Fluorescence

ABSTRACT

For organnoboron compounds, the substituents on boron atoms are very important because they not only impact on the molecular stability but also significantly modulate the electronic structures and properties. In this manuscript, we synthesized two new B←N-containing azaacenes with propynyl groups on boron atoms through one-step Grignard reaction. Replacing fluorine atoms by propynyl groups greatly impacts on the electronic energy levels, especially enhancing the HOMO levels, thus leading to the narrowed HOMO-LUMO bandgaps. These B←N-containing azaacenes exhibit the NIR light-absorption ($\lambda_{abs}$ = 706 nm for **2a** and 762 nm for **2b**) and fluorescence properties ($\lambda_{em}$ = 740 nm for **2a** and 802 nm for **2b**), as well as multiple reversible redox behaviors, which are significantly different from the analogs with fluorine atoms. This study thus provides a functional substituent of boron atom, which may lead to new organoboron materials with fascinating properties.



Boron-containing $\pi$-electron systems, which integrate $sp^2$-hybridized carbon skeleton and boron atoms, have drawn much attention in both synthetic chemistry and material science [1–6]. Till now, many B-containing $\pi$-systems have been developed for various optical and electronic applications, such as emissive materials in organic light-emitting devices (OLEDs), electron acceptors in organic solar cells (OSCs), semiconductors in organic field-effect transistors (OFETs), and electrode materials in lithium batteries, *etc.* [7–15]. In design of B-containing $\pi$-systems, the substituents on boron atoms are very important because they not only impact on the stability of the compounds but also significantly modulate the electronic structures and properties [16–24]. For example, the bulky aryl groups are usually incorporated into tricoordinate B-containing compounds to sterically protect the boron atom due to its intrinsic instability towards oxygen and moisture. The substituents of tetracoordinate B-containing compounds can tune their light-absorption and fluorescence properties as well as electrochemical properties. Therefore, the development of new substituents on boron atom and investigation of their effects on $\pi$-systems remain crucial for organoboron chemistry and materials.

$\pi$-Systems containing boron-nitrogen coordination bond (B←N) as a typical kind of tetracoordinate organoboranes have received particular attention, because they have shown many intriguing properties, such as photo/thermo-chromism, thermally activated delayed fluorescence (TADF), and electron-transporting behavior [25–29]. Notably, B←N unit has been used to design n-type organic and polymer semiconductors for organic electronic applications [30–33]. For instance, two B←N-containing azaacenes with the fluorine atoms on boron atoms (**1a** and **1b** in Scheme 1) have been developed, which exhibited low-lying LUMO/HOMO energy levels ($E_{LUMO}/E_{HOMO}$) and excellent electron-transporting performance in OFETs [34].

In this communication, we report that nucleophilic substitution reaction could proceed on **1a** and **1b**, producing two new B←N-containing azaacenes (**2a** and **2b**) with the propynyl groups on boron atoms. They are good candidates to investigate the effects of the propynyl groups on $\pi$-systems. The theoretical and experimental results demonstrate that replacing fluorine atoms by propynyl groups significantly enhances the electronic energy levels, especially HOMO levels, and leads to some attractive optoelectronic properties, such as the near-infrared (NIR) light-absorption and fluorescence properties, as well as multiple reversible redox behaviors. The details are presented herein.

Scheme 1 shows the synthesis of **2a** and **2b**, through one-step Grignard reaction with 1-propynylmagnesium bromide. The nucleophilic substitution reactions proceeded completely on **1a** and **1b**, producing **2a** and **2b** in the yields of over 70% after purification by silica gel column chromatography [35]. The chemical structures of **2a** and **2b** are unambiguously characterized by $^1$H and $^{13}$C NMR spectra and elemental analysis. **2a** and **2b** are

* Corresponding authors.
*E-mail addresses:* gaoying@cust.edu.cn (Y. Gao), chuandong.dou@ciac.ac.cn (C. Dou), liujun@ciac.ac.cn (J. Liu).

https://doi.org/10.1016/j.cclet.2019.11.018

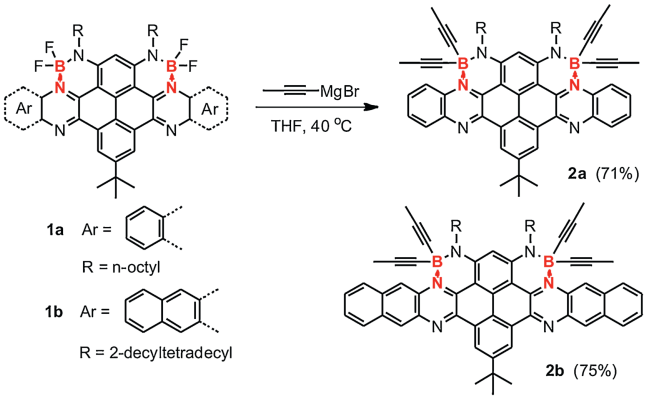


**Scheme 1.** Synthesis of **2a** and **2b**.

easily soluble in common organic solvents (> 20 mg/mL), such as chloroform, tetrahydrofuran and toluene, suggesting that the propynyl substituents can enhance the solubility of organoboron compounds. Thermogravimetric analysis (TGA) was used to characterize the thermal stability of **2a** and **2b** under nitrogen atmosphere. Upon increasing the temperature, an obvious weight loss of 8% at 273 °C was observed for **2a** (Fig. S1 in Supporting information). Similarly, **2b** exhibits a weight loss of 5% at 240 °C. As calculated, the weight losses of **2a** and **2b** are ascribed to the release of two propynyl groups (theoretical values: 8.7% for **2a** and 5.4% for **2b**).

B←N-containing azaacenes with the propynyl groups display the interesting photophysical properties. The detailed data of **2a** and **2b** as well as **1a** and **1b** are summarized in Table 1. The solutions of **2a** and **2b** in toluene are deep blue and purple, respectively. As shown in Fig. 1a, the characteristic absorption bands in 300–800 nm are observed in their UV–vis spectra. While **2a** shows the maximum absorption peaks ($\lambda_{abs}$) at 706/647 nm, **2b** exhibits the $\lambda_{abs}$ at 762/692 nm. The molar absorption coefficient is $8.40 \times 10^4$ L mol$^{-1}$ cm$^{-1}$ for **2a** and $1.17 \times 10^5$ L mol$^{-1}$ cm$^{-1}$ for **2b**, respectively. The redshifted absorption by ca. 50 nm from **2a** to **2b** and the higher light-absorption ability of **2b** are attributed to the extended $\pi$-conjugation of **2b**. These NIR absorption properties are rarely observed in organoboron compounds, which are mostly based on 4,4′-difluoro-4-bora-3a,4a-diaza-s-indacene (BODIPY) [36,37]. Moreover, in comparison to **1a** and **1b**, **2a** and **2b** show the red-shifted absorption spectra by as large as *ca.* 70 nm, respectively, indicating that replacing fluorine atoms by propynyl groups on boron atoms greatly impacts on the absorption properties of B-containing conjugated molecules.

The fluorescence spectra of **2a** and **2b** exhibit the main emission bands in the NIR region with the peak maxima ($\lambda_{em}$) at 740 nm for **2a** and 802 nm for **2b** (Fig. 1b), respectively, although their fluorescence quantum yields ($\Phi$) are moderate. The fluorescence peaks of **2a** and **2b** are significantly red-shifted by *ca.* 90 nm

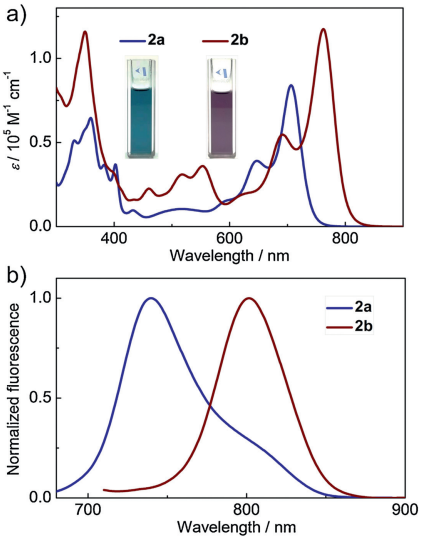


**Fig. 1.** (a) UV–vis absorption spectra and (b) fluorescence spectra of **2a** and **2b** in toluene. Insets are the photographs of the two solutions.

comparing with that of **1a** and **1b**. In addition, negligible solvent effects are shown in the fluorescence spectra of **2a** and **2b** as well as their absorption spectra (Figs. S3, S5 and S6 in Supporting information).

To illustrate the electronic effects of the propynyl groups, we performed density functional theory (DFT) calculations at the B3LYP/6-31 G(d,p) level of theory. The model compounds **2a-Me** and **2b-Me** with methyl groups were adopted for simplified calculations. The optimized structures of **2a-Me** and **2b-Me** both display the fully planar frameworks with four pendant propynyl groups (Fig. S7 in Supporting information). While the LUMOs of **2a-Me** and **2b-Me** are localized on the azaacene skeletons, the HOMOs are mainly distributed on the electron-rich alkylamine-linked phenyl rings and the peripheral rings of azaacene skeletons (Fig. 2). These LUMOs and HOMOs are quite similar to that of **1a-Me** and **1b-Me**, respectively, which have been reported in the previous work. It indicates that replacing fluorine atoms by propynyl groups has few effects on the molecular orbital distributions. Notably, in comparison to **1a-Me** and **1b-Me**, **2a-Me** and **2b-Me** exhibit the enhanced LUMO and HOMO energy levels, respectively, especially HOMO levels, thus leading to the narrow HOMO-LUMO bandgaps. This is ascribed to the weak electron-accepting character of the propynyl group, which significantly impacts on the HOMO levels of organoboron compounds.

Time-dependent DFT calculations were conducted to illustrate the absorption properties of **2a** and **2b**. As shown in Fig. 2, the absorption bands at 706 and 647 nm of **2a** are both assignable to the HOMO→LUMO and HOMO−1→LUMO+1 transitions. For **2b**, the absorption bands at 762 nm and 692 nm are assigned to the

**Table 1**
The photophysical and electrochemical properties of **2a** and **2b** as well as **1a** and **1b**.

| Compd. | $\lambda_{abs}$ (nm) [a] | $\varepsilon_{max}$ (L mol$^{-1}$ cm$^{-1}$)[a] | $\lambda_{em}$ (nm) [a] | $\Phi$[a] | $E^{red}$ (V) [b] | $E^{ox}$ (V) [b] | $E_{LUMO}$ (eV) [d] | $E_{HOMO}$ (eV) [d] |
|---|---|---|---|---|---|---|---|---|
| **2a** | 706/647 | $8.40 \times 10^4$ | 740 | 0.06 | −1.24/−1.72/−2.18 | +0.58/+1.09 | −3.56 | −5.38 |
| **2b** | 762/692 | $1.17 \times 10^5$ | 802 | 0.02 | −1.08/−1.53/−1.99 | +0.63 | −3.72 | −5.43 |
| **1a** | 635/587 | $9.48 \times 10^4$ | 654 | 0.05 | −1.10/−1.70 | +1.07[c] | −3.70 | −5.87 |
| **1b** | 686/628 | $1.13 \times 10^5$ | 705 | 0.02 | −0.93/−1.48 | +1.07[c] | −3.87 | −5.87 |

[a] Measured in toluene solution.
[b] Reduction/oxidation potentials *versus* Fc/Fc$^+$.
[c] Anodic peak potential.
[d] Calculated using the equation of $E_{HOMO}/E_{LUMO} = -(4.80 + E^{ox1}/E^{red1})$ eV.

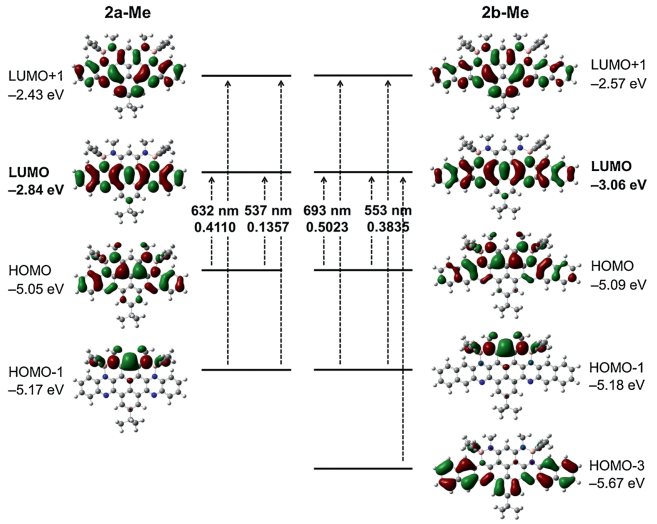


**Fig. 2.** Selected Kohn-Sham molecular orbitals and energy diagrams, as well as excitation energies and oscillator strengths of **2a** and **2b** calculated by DFT and TD-DFT at the B3LYP/6-31 G(d,p) level, respectively.

HOMO→LUMO and HOMO−1→LUMO+1 transitions and the HOMO→LUMO, HOMO−1→LUMO+1 and HOMO−3→LUMO transitions (Figs. S8 and S9 in Supporting information). The absorption spectra of **2a** and **2b** are well reproduced by the TD-DFT calculations, which all involve the HOMO→LUMO transitions. Namely, the NIR absorption properties of B←N-containing azaacenes with the propynyl groups are closely related to the narrowed HOMO-LUMO bandgaps. These calculations demonstrate that the electronic energy levels and absorption properties of organoboron compounds can be tuned through the incorporation of the propynyl groups on boron atoms.

To experimentally gain insight into the electronic properties, we measured the cyclic voltammetry of B←N-containing azaacenes **2a** and **2b** in $CH_2Cl_2$. Both of them show three reversible reduction processes, accompanying with two reversible oxidation processes for **2a** and one reversible oxidation process for **2b**. In contrast, **1a** and **1b** with fluorine atoms display the reversible reduction processes and the irreversible oxidation processes. It is suggested that the propynyl groups in **2a** and **2b** can stabilize not only the generated radical anion intermediates but also the resulted radical cation intermediates. The first half-wave reduction and oxidation potentials ($E^{red1}/E^{ox1}$ *vs.* $Fc/Fc^+$) are −1.24/+0.58 V for **2a** and −1.08/+0.63 V for **2b**. According to the equation of $E_{LUMO}/E_{HOMO} = -(4.80 + E^{red1}/E^{ox1})$, the experimental $E_{LUMO}$ and $E_{HOMO}$ of **2a** and **2b** are calculated to be −3.56/−5.38 eV and −3.72/−5.43 eV, respectively. The $E_{LUMO}$ and $E_{HOMO}$ of **2a** are higher than that of **1a** by 0.14 and 0.49 eV, respectively. Similarly, The $E_{LUMO}$ and $E_{HOMO}$ of **2b** are enhanced by 0.15 eV and 0.44 eV from that of **1b**. These changes are fully consistent with the theoretical calculation results. Thus, replacing fluorine atoms by propynyl groups plays an important role in tuning the electronic energy levels, especially enhancing the HOMO levels (Fig. 3).

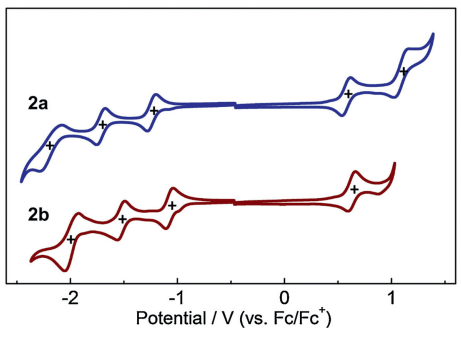


**Fig. 3.** Cyclic voltammograms of **2a** and **2b** in $CH_2Cl_2$ (0.4 mmol/L). Fc = ferrocene.

In summary, we synthesized two new B←N-containing azaacenes with the propynyl groups on boron atoms through one-step Grignard reaction. The replacement of fluorine atoms by propynyl groups greatly impacts on the electronic energy levels, especially enhancing the HOMO levels, thus leading to the narrowed HOMO-LUMO bandgaps. These B←N-containing azaacenes with the propynyl groups exhibit the NIR light-absorption and fluorescence properties, as well as multiple reversible redox behaviors, which are significantly different from the analogs with fluorine atoms. This study thus provides a functional substituent of boron atom, which may lead to new organoboron materials with fascinating properties.

## Declaration of competing interest

The authors declare that they have no known competing financial interests or personal relationships that could have appeared to influence the work reported in this paper.

## Acknowledgments

This work was supported by the National Natural Science Foundation of China (Nos. 21822507, 21625403, 21761132020), National Key Research and Development Program of China (No. 2018YFE0100600), founded by MOST, Youth Innovation Promotion Association of Chinese Academy of Sciences (No. 2017265).

## Appendix A. Supplementary data

Supplementary material related to this article can be found, in the online version, at doi:https://doi.org/10.1016/j.cclet.2019.11.018.

## References

[1] M. Hirai, N. Tanaka, M. Sakai, S. Yamaguchi, Chem. Rev. 119 (2019) 8291–8331.
[2] D. Frath, J. Massue, G. Ulrich, R. Ziessel, Angew. Chem. Int. Ed. 53 (2014) 2290–2310.
[3] A. Lorbach, A. Hübner, M. Wagner, Dalton Trans. 41 (2012) 6048–6063.
[4] S.K. Mellerupab, S. Wang, Chem. Soc. Rev. 48 (2019) 3537–3549.
[5] Y. Ren, F. Jäkle, Dalton Trans. 45 (2016) 13996–14007.
[6] P.G. Campbell, A.J.V. Marwitz, S.Y. Liu, Angew. Chem. Int. Ed. 51 (2012) 6074–6092.
[7] D. Li, H. Zhang, Y. Wang, Chem. Soc. Rev. 42 (2013) 8416–8433.
[8] Y.L. Rao, S. Wang, Inorg. Chem. 50 (2011) 12263–12274.
[9] Z.D. Zhuang, Z.H. Sun, Z.F. Yao, Q.R. Chen, Angew. Chem. Int. Ed. 58 (2019) 10708–10712.
[10] X.Y. Wang, F.D. Zhuang, R.B. Wang, X.C. Wang, et al., J. Am. Chem. Soc. 136 (2014) 3764–3767.
[11] W.B. Liu, M. Li, L. Fang, C.F. Chen, Chin. Chem. Lett. 29 (2018) 40–46.
[12] W. Zhang, G. Li, L. Xu, Y. Zhuo, et al., Chem. Sci. 9 (2018) 4444–4450.
[13] L. Wang, K.Q. Ye, H.Y. Zhang, Chin. Chem. Lett. 27 (2016) 1367–1375.
[14] C. Dou, J. Liu, L. Wang, Sci. China Chem. 60 (2017) 450–459.
[15] C. Duan, G. Zango, M.G. Iglesias, F.J.M. Colberts, Angew. Chem. Int. Ed. 56 (2017) 148–152.
[16] L. Ji, S. Griesbeck, T.B. Marder, Chem. Sci. 8 (2017) 846–863.
[17] S. Yamaguchi, T. Shirasaka, S. Akiyama, K. Tamao, J. Am. Chem. Soc. 124 (2002) 8816–8817.
[18] L.G. Mercier, W.E. Piers, M. Parvez, Angew. Chem. Int. Ed. 48 (2009) 6108–6111.
[19] A.Jr. Caruso, M.A. Siegler, J.D. Tovar, Angew. Chem. Int. Ed. 49 (2010) 4213–4217.
[20] T. Wang, C. Dou, J. Liu, L. Wang, Chem. -Eur. J. 24 (2018) 13043–13048.
[21] M. Grandl, B. Rudolf, Y. Sun, D.F. Bechtel, et al., Organometallics 36 (2017) 2527–2535.
[22] M. Grandl, Y. Sun, F. Pammer, Org. Chem. Front. 5 (2018) 336–352.
[23] D.L. Crossley, I.A. Cade, E.R. Clark, A. Escande, et al., Chem. Sci. 6 (2015) 5144–5151.
[24] X. Shao, C. Dou, J. Liu, L. Wang, Sci. China Chem. 62 (2019) 1387–1392.
[25] A. Wakamiya, T. Taniguchi, S. Yamaguchi, Angew. Chem. Int. Ed. 45 (2006) 3170–3173.

[26] Y.L. Rao, H. Amarne, S.B. Zhao, T.M. McCormick, et al., J. Am. Chem. Soc. 130 (2008) 12898–12900.
[27] K. Liu, R.A. Lalancette, F. Jäkle, J. Am. Chem. Soc. 139 (2017) 18170–18173.
[28] K. Matsuo, T. Yasuda, Chem. Commun. (Camb.) 53 (2017) 8723–8726.
[29] Y.J. Shiu, Y.C. Cheng, W.L. Tsai, C.C. Wu, et al., Angew. Chem. Int. Ed. 55 (2016) 3017–3021.
[30] C. Dou, Z. Ding, Z. Zhang, Z. Xie, et al., Angew. Chem. Int. Ed. 54 (2015) 3648–3652.
[31] R. Zhao, C. Dou, J. Liu, L. Wang, et al., Chin. J. Polym. Sci. 35 (2017) 198–206.
[32] X. Long, C. Dou, J. Liu, L. Wang, Chin. Chem. Lett. 29 (2018) 1343–1346.
[33] Y. Min, C. Dou, H. Tian, J. Liu, et al., Chem. Commun. (Camb.) 55 (2019) 3638–3641.
[34] Y. Min, C. Dou, H. Tian, Y. Geng, et al., Angew. Chem. Int. Ed. 57 (2018) 2000–2004.
[35] L.J. Patalag, P.G. Jones, D.B. Werz, Angew. Chem. Int. Ed. 55 (2016) 13340–13344.
[36] Y. Ni, S. Lee, M. Son, N. Aratani, et al., Angew. Chem. Int. Ed. 55 (2016) 2815–2819.
[37] G.M. Fischer, E. Daltrozzo, A. Zumbusch, Angew. Chem. Int. Ed. 50 (2011) 1406–1409.